Published in final edited form as:

*J Thromb Haemost*. 2021 September ; 19(9): 2182–2192. doi:10.1111/jth.15430.

# The contribution of TFPIα to the hemostatic response to injury in mice

**Tanya T. Marar**[1], **Nicholas D. Martinez**[2], **Susan A. Maroney**[2], **Amy E. Siebert**[2], **Jie Wu**[1], **Timothy J. Stalker**[1], **Maurizio Tomaiuolo**[1], **Sinny Delacroix**[3], **Robert D. Simari**[4], **Alan E. Mast**[2,5], **Lawrence F. Brass**[1]

[1]Department of Medicine, Perelman School of Medicine, University of Pennsylvania, Philadelphia, PA, USA

[2]Versiti Blood Research Institute, Milwaukee, WI, USA

[3]Department of Medicine, University of Adelaide, Adelaide, Australia

[4]Department of Cardiovascular Medicine, University of Kansas School of Medicine, Kansas City, KS, USA

[5]Department of Cell Biology, Neurobiology, and Anatomy, Medical College of Wisconsin, Milwaukee, WI, USA

## Abstract

**Background:** Tissue factor pathway inhibitor (TFPI) is an essential regulator of coagulation, limiting thrombin generation and preventing thrombosis. In humans and mice, TFPIα is the sole isoform present in platelets.

**Objective:** Here, we asked whether TFPIα, because of its release from platelets at sites of injury, has a unique role in limiting the hemostatic response.

**Methods:** TFPIα-mutant (*Tfpi*$^{\Delta\alpha/\Delta\alpha}$) mice were generated by introducing a stop codon in the C-terminus. Platelet accumulation, platelet activation, and fibrin accumulation were measured following penetrating injuries in the jugular vein and cremaster muscle arterioles, and imaged by fluorescence and scanning electron microscopy. Time to bleeding cessation was recorded in the jugular vein studies.

**Correspondence**: Lawrence F. Brass, Perelman School of Medicine, Philadelphia, PA 19104, USA. brass@pennmedicine.upenn.edu, Alan E. Mast, Versiti Blood Research Institute, PO Box 2178, Milwaukee, WI 53201-2178, USA. aemast@versiti.org.

AUTHOR CONTRIBUTIONS

Tanya T. Marar: Designed, performed research, analyzed and interpreted data, and wrote the manuscript. Nicholas D. Martinez: Maintained and genotyped mice, performed plasma and platelet lysate assays. Susan A. Maroney: Designed and interpreted experiments, and wrote the manuscript. Amy E. Siebert: Analyzed and interpreted data, and wrote the manuscript. Jie Wu: Performed cremaster muscle injury model. Timothy J. Stalker: Designed and interpreted experiments, and wrote the manuscript. Maurizio Tomaiuolo: Designed and interpreted experiments, performed scanning electron microscopy, and wrote the manuscript. Sinny Delacroix: Created the TFPIα-deficient mouse line. Robert D. Simari: Provided the TFPIα-deficient mouse line. Alan E. Mast: Designed and interpreted experiments, and wrote the manuscript. Lawrence F. Brass: Designed and interpreted experiments, and wrote the manuscript.

SUPPORTING INFORMATION

Additional supporting information may be found online in the Supporting Information section.

**Results:** *Tfpi*$^{\Delta\alpha/\Delta\alpha}$ mice were viable and fertile. Plasma TFPI levels were normal in the *Tfpi*$^{\Delta\alpha/\Delta\alpha}$ mice, no TFPI protein or activity was present in their platelets and thrombin-antithrombin complex levels were indistinguishable from *Tfpi*$^{+/+}$ littermates. There was a small, but statistically significant reduction in the time to bleeding cessation following jugular vein puncture injury in the *Tfpi*$^{\Delta\alpha/\Delta\alpha}$ mice, but no measurable changes in platelet or fibrin accumulation or in hemostatic plug architecture following injury of the micro- or macrovasculature.

**Conclusion:** Loss of TFPIα expression does not produce a global prothrombotic state in mice. Platelet TFPIα is expected to be released or displayed in a focal manner at the site of injury, potentially accumulating to high concentrations in the narrow gaps between platelets. If so, the data from the vascular injury models studied here indicate this is not essential for a normal hemostatic response in mice.

### Keywords

anticoagulant; hemostasis; platelets; TFPIα; tissue factor pathway inhibitor

## 1 | INTRODUCTION

Tissue factor pathway inhibitor (TFPI) is a primary anticoagulant regulating the hemostatic response to vascular injury when coagulation is initiated via tissue factor (TF) exposure. It also appears to be essential for normal development because there are no reports of humans that lack TFPI and mice engineered to lack TFPI die *in utero*.[1] TFPI regulates coagulation in part by binding to and blocking the active sites of factors Xa (FXa) and VIIa (FVIIa) simultaneously after FX is activated by TF-VIIa complexes.[2,3] This limits further TF-dependent generation of FXa, reducing the amount of thrombin that can be generated.[2,3] TFPIα can also inhibit early prothrombinase complexes assembled with forms of FVa that retain portions of the factor V (FV) B-domain.[4] This includes forms produced when FV is cleaved by FXa,[5] partially proteolyzed forms of FVa released from platelets,[6] and forms produced from transcripts containing a mutation causing alternative splicing within the B-domain.[4,7–10]

The three known isoforms of TFPI are synthesized from alternatively spliced transcripts of a single gene that vary in structure and localization, as well as between species. TFPI protein is expressed as α and β isoforms in humans and α, β, and γ in mice.[11–15] All TFPI isoforms consist of an acidic amino terminus followed by two Kunitz-type serine protease inhibitor domains, termed K1 and K2. The structural differences between isoforms occur after the K2 domain.[16] TFPIα contains a third Kunitz domain (K3) followed by a basic C-terminus. TFPIβ lacks K3 but has a glycosyl phosphatidylinositol anchor for membrane association.[13] TFPIγ lacks K3 and has a carboxyl terminus after K2 encoding a soluble protein that is detectable in plasma.[11] K1 and K2 bind to and inhibit the active site of FVIIa and FXa, respectively. K3 binds protein S, which then acts as a cofactor for inhibiting FXa.[17,18] The C-terminus of TFPIα is needed for efficient inhibition of FXa[19] and also binds to FVa allowing it to inhibit early forms of prothrombinase.[9,17,18] Of the various isoforms, TFPIα has the greatest inhibitory activity when soluble protein is added to *in vitro* coagulation assays, reflecting the contribution of all three Kunitz domains and the basic C-terminus to its

anticoagulant activity.[19,20] However, TFPIβ associated with a cell surface inhibits TF-FVIIa at rates equivalent to soluble TFPIα.[16]

Tissue and plasma TFPI isoforms and concentrations differ in humans and mice. The α and β isoforms are variably expressed by cultured human endothelial cells.[21] TFPIβ is the predominant isoform present on the surface of murine endothelium and is likely the predominant form on human endothelium as well.[22–26] Platelets, on the other hand, contain exclusively TFPIα in both humans and mice that is synthesized in megakaryocytes rather than being endocytosed from plasma.[27,28] In addition, TFPI has been found in monocytes/macrophages, vascular smooth muscle cells, and cardiac myocytes.[25–27,29–33] Tandem mass spectrometry detects the α and β isoforms in human plasma and the α and γ isoforms in mouse plasma.[34] In humans, the plasma TFPIα concentration is ~0.2 to 0.4 nM, increasing 2- to 4-fold following heparin infusion which suggests that a substantial fraction is bound to vascular glycosaminoglycans.[35–38] In mice, the plasma TFPIα concentration is lower than in humans and difficult to detect, but it does increase slightly following heparin infusion.[23,34,39] However, despite the minimal presence of TFPIα, the total concentration of TFPI in mouse plasma is ~20 times greater than in human plasma. The difference is due to the high concentration of TFPIγ in mouse plasma.

Given the isoform-selective abilities of TFPIα to bind protein S and FVa and inhibit prothrombinase,[17,19,40] it is worth considering whether the TFPIα that is carried by platelets has a special role, especially because it would be expected to be released and potentially accumulate when platelets are activated at the site of injury.[28] Previous studies have suggested that this may be the case. In those studies, chimeric mice lacking hematopoietic TFPI were generated by transplanting fetal liver cells from mice lacking the TFPI K1 domain (*Tfpi*$^{tm1Gjb}$; *Tfpi*$^{-/-}$) into lethally irradiated *Tfpi*$^{+/-}$ mice. Thrombus growth was studied in the femoral vein and carotid artery using an electrolytic injury model. The results showed greater platelet accumulation in the mice lacking hematopoietic TFPI, just as would be expected if TFPIα carried by platelets normally suppresses thrombin production.[41] Removing hematopoietic TFPI also reduced bleeding in FVIII-deficient mice.[42] Notably, however, the chimeric mice used in those studies not only had reduced expression of TFPI in hematopoietic cells, but also had a 50% reduction in TFPI expression because they were produced in a *Tfpi*$^{+/-}$ background. This decrease in plasma TFPI levels complicates the interpretation of the results.

Here, we have tested the hypothesis that TFPIα in general and platelet TFPIα in particular has a special role in regulating the hemostatic response, using transgenic mice that have a selective defect in TFPIα expression (denoted *Tfpi*$^{\Delta\alpha/\Delta\alpha}$). *Tfpi*$^{\Delta\alpha/\Delta\alpha}$ mice were produced by introducing a premature stop codon in the TFPI C-terminal domain, a change that prevented the expression of the protein rather than producing a truncated protein. In the present study, we characterized platelets and plasma TFPI expression in the *Tfpi*$^{\Delta\alpha/\Delta\alpha}$ mice and determined if they had a global prothrombotic state. We also asked whether loss of TFPIα altered the kinetics or composition of the hemostatic response using two previously described models of penetrating injury in the microvasculature[43] and macrovasculature.[44] The results show that loss of TFPIα produced a small but statistically significant decrease in the time to bleeding cessation following jugular vein puncture injury, but no apparent

changes in either the structure of the hemostatic plug produced in the jugular vein or the kinetics and structure of the hemostatic plug formed in the cremaster muscle microcirculation.

## 2 | METHODS AND MATERIALS

### 2.1 | Animals

B6.Cg-Tg(ACTFLPe)9205Dym/J (Stock No: 005703; ACTB-Flpe) mice and C57BL/6J (Stock No: 000664; B6J) mice were obtained from the Jackson Laboratory (Bar Harbor, ME). Mice carrying the *Tfpi*$^{\Delta\alpha}$ allele were generated by targeted insertion of a premature stop codon at the 5′-end of the TFPIα isoform-specific terminal exon encoding the basic C-terminus (Figure 1A and B). Two fragments of genomic DNA were amplified from the murine *Tfpi* locus and inserted into the pNTKV1901-frt/*lox*P vector backbone.[45,46] These fragments included a 4600-bp 5′ homology arm sequence containing *Tfpi* exon 8 (based on the NM_011576.1 reference sequence) and a 4590-bp 3′ homology arm sequence containing exon 9. The in-frame premature stop codon within exon 9 (c.835–837delins* (p.L279X)) was incorporated using polymerase chain reaction (PCR)-based site-directed mutagenesis. The final targeting vector included an ~1770-bp sequence that contained a Pgk-Neo resistance cassette flanked by two Frt sites and a single 3′-loxP site positioned within the intron between exons 8 and 9 of *Tfpi* (Figure 1B). The linearized targeting vector was electroporated into pluripotent 129 Sv/J embryonic stem cells, and clones carrying the construct were identified by neomycin selection. *Tfpi*$^{+/\Delta\alpha}$ mice were backcrossed for 7 generations to the B6J genetic background. Removal of the Pgk-Neo cassette within intron 8 of the *Tfpi*$^{\Delta\alpha}$ allele was accomplished by outcrossing *Tfpi*$^{+/\Delta\alpha}$ mice to homozygous ACTB-Flpe mice for Flp-mediated recombination between the flanking Frt sites (Figure 1B). All comparisons were performed using littermates produced by breeding *Tfpi*$^{+/\Delta\alpha}$ mice. The Institutional Animal Care and Use Committees of the University of Pennsylvania and the Medical College of Wisconsin approved all procedures.

### 2.2 | Genotypic analysis

Genomic DNA was isolated from ear biopsies and used for genotyping by PCR analysis. The sequences of the primer pairs are as follows: TFPI CT del FOR: 5′—ACC AGA AGG AGA TGT CTG AG—3′ and TFPI CT del REV: 5′—GGA CCT GAT ACC CGA CTT G-3′. The PCR cycling conditions were as follows: 2 min at 95°C followed by 35 cycles of 30 s at 95°C, 30 s at 56.6°C, and 35 s at 72°C, and a final 5 min at 72°C. The PCR product derived from the wild-type allele is 380 bp, heterozygote is 380 bp and 426 bp, and that derived from the homozygote mutant is 426 bp. PCR products were analyzed by gel electrophoresis on 1.5% agarose gels.

### 2.3 | Plasma and platelet isolation

Whole blood was collected from the inferior vena cava into 3.2% citrate (10% vol/vol) from male and female mice. Platelet-poor plasma was prepared by consecutive 10-min centrifugation at 3000*g* and 9000*g*. Platelet lysates were prepared from platelet-rich plasma from two genetically identical mice and pooled by collecting the upper 1/3 of whole blood after centrifugation (100*g*, 5 min), followed by centrifugation of each platelet-enriched

plasma fraction (100*g*, 5 min). Platelets were pelleted (700*g*, 10 min), washed three times with phosphate-buffered saline, and lysed by repeated freeze thaw (5×) followed by sonication (Bioruptor Pico sonicator; Diagenode Inc, Denville, NJ).

### 2.4 | Measurement of TFPI activity

Assays were performed with plasma diluted 1:200 or with platelet lysates standardized to contain 750 μg total protein/ml using the bicinchoninic acid assay (ThermoScientific, Waltham, MA). Samples with or without addition of 50 nM polyclonal rabbit anti-mouse TFPI antibody[23,39,41,46–48] were incubated for 20 min with 1:500 rabbit brain cephalin (Pel-Freez Biologicals, Rogers, AK), 0.001 nM human FVIIa (Novo Nordisk A/S, Bagsvaerd, DK) and 1:4000 human TF (Siemens, Marburg, Germany). Spectrozyme FXa (0.5 mM, Sekisui Diagnostics, Stamford, CT) was added and reactions initiated with 20 nM human FX (Enzyme Research Labs, South Bend, IN). FXa generation was measured at 405 nm for 1 h using SoftMax Pro, version 4.3.1. Plasma and platelet TFPI activity was interpolated from standard curves using GraphPad Prism 9.1.0 using nonlinear regression parameters. Standard curves for plasma assays were generated using a 10-point series of B6J wild-type plasma diluted to contain different percentages of TFPI using TFPI-deficient plasma obtained from *Tfpi*$^{-/-}$ *F2rl3*$^{-/-}$ mice.[49] Plasma TFPI activity is presented as percent B6J wild-type plasma activity. Standard curves for platelet lysate assays were generated using a twofold dilution series of murine recombinant TFPIα (Novo Nordisk A/S, Bagsvaerd, DK). Platelet TFPIα activity is presented as femtomoles TFPIα per mg total platelet protein.

### 2.5 | Mouse plasma TFPI ELISA

Total mouse TFPI was measured in plasma samples (1:4000) with a previously described ELISA[41] modified for detection of the TFPI/antibody complex (polyclonal rabbit anti-mouse TFPI antibody) using a horseradish peroxidase-conjugated donkey anti-rabbit secondary antibody (Jackson Immunoresearch Laboratory, West Grove, PA) and the QuantaRed Enhanced chemifluorescent horseradish peroxidase substrate (ThermoScientific) following manufacturer's instructions. Substrate cleavage kinetics over 15 min were measured on the EnSpire Workstation Version 4.10 (PerkinElmer, Inc., Waltham, MA).

### 2.6 | Western blot analysis

Platelet lysates were examined for TFPIα by western blot with a rabbit anti-mouse TFPI polyclonal antibody following precipitation with FXa as previously described.[23]

### 2.7 | Quantitation of thrombin-antithrombin complexes

Thrombin-antithrombin (TAT) complexes were quantified in platelet-poor plasma according to the manufacturer's instructions (mouse thrombin-antithrombin complexes ELISA kit, Abcam, Cambridge, MA).

### 2.8 | Jugular puncture injury model

Hemostatic plug formation following puncture injury in a mouse jugular vein was performed according to the procedure by Tomaiuolo et al.[44] The right external jugular vein was isolated and gently cleaned of connective tissue. After infusion of fluorescently labeled imaging

reagents, a puncture injury was created in the vein using a 30-gauge needle (300 μm diameter), which resulted in bleeding. Extravasated blood was continually rinsed away from the injury site by slow superfusion of normal saline delivered via a syringe pump. The time to cessation of bleeding, as visualized through a dissecting microscope, was recorded as bleeding time. The hemostatic response was stopped at 5 min postinjury via transcardiac perfusion of sodium cacodylate buffer (0.2 M sodium cacodylate, 0.15 M sodium chloride at pH 7.4), followed by perfusion of 4% paraformaldehyde. After perfusion, the vein was excised, placed in a 35-mm dish coated with silicone, and submerged in paraformaldehyde. The vein was then carefully cleaned of any remaining connective tissue, cut along its length, opened, and pinned to the silicone pad with the intraluminal or extravascular portion of the injury site of the vessel surface up. The vessel remained in fixative at 4°C until fluorescence imaging was performed.

### 2.9 | Cremaster muscle injury model

Hemostatic plug formation was visualized in the cremaster muscle microcirculation of male mice according to Stalker et al.[43] Male mice 8 to 12 weeks of age were anesthetized via intraperitoneal injection of ketamine (100 mg/kg)/xylazine (10 mg/kg)/acepromazine (3 mg/kg). The cremaster muscle was exteriorized, cleaned of connective tissue, opened, and spread flat on the glass coverslip of a custom-built chamber for viewing by intravital microscopy. The cremaster preparation was continuously superfused with bicarbonate buffer warmed to 36.5°C and bubbled with 95% $N_2$/5% $CO_2$. The cremaster microcirculation was visualized using an Olympus BX61WI upright microscope with a 60X (0.9 NA) water immersion objective, coupled to a Yokogawa CSU-X1 spinning disk confocal scanner. Diode pumped solid state lasers (488, 568, 640 nm) with AOTF control were used as the fluorescence excitation light source (LaserStack, Intelligent Imaging Innovations, Denver, CO). Confocal fluorescence images were acquired using an Evolve EM-CCD digital camera (Photometrics, Tucson, AZ). The microscope, confocal scanner, lasers, and camera were all controlled and synchronized using Slidebook 6.0 image acquisition and analysis software (Intelligent Imaging Innovations). A total of 30- to 40-μm diameter arterioles with unperturbed blood flow were selected for study. Anti-CD41 F(ab)2 fragments (0.12 μg/g body weight; clone MWReg30, BD Bioscience), anti-P-selectin (0.2 μg/g body weight; clone RB40.34, BD Bioscience), and anti-fibrin (0.2 μg/g body weight; clone 59D8) were infused intravenously via the jugular vein. Antibodies were labeled with Alexa fluor dye monoclonal antibody labeling kits (Alexa-488, Alexa-568, and Alexa-647) according to the manufacturer's instructions (Invitrogen).

### 2.10 | Statistics

Statistical analyses comparing results from plasma and platelet ELISA and activity assays were performed with GraphPad Prism Version 9.1.0.

## 3 | RESULTS

### 3.1 | Generation of TFPIα-deficient mice

Mice carrying the *Tfpi*$^{\Delta\alpha}$ allele were generated using the pNTKV-frt/loxp vector backbone[45,46] for targeted insertion of a premature stop codon at the 5′-end of the TFPIα

isoform-specific terminal exon encoding the basic C-terminus (Figure 1A and B). These mice were originally intended for a study on the role of the TFPIα C-terminal domain but, as shown below, the stop codon resulted in total loss of platelet TFPIα expression. DNA analysis of 426 off-spring produced by intercrossing the resulting *Tfpi*$^{+/\Delta\alpha}$ mice revealed a normal Mendelian genotype distribution (Table 1). *Tfpi*$^{+/\Delta\alpha}$ and *Tfpi*$^{\Delta\alpha/\Delta\alpha}$ mice developed normally and reached adulthood. There were no significant differences in hematocrit, leukocyte counts, or platelet count (Table 2). Immunoblot analysis, using a rabbit anti-mouse polyclonal antibody directed against the full-length protein,[28,50] indicated that TFPIα expression in platelet lysates was reduced in the *Tfpi*$^{+/\Delta\alpha}$ mice and undetectable in the *Tfpi*$^{\Delta\alpha/\Delta\alpha}$ mice (Figure 1D). Notably, the antibody used for this western blot was able to recognize recombinant TFPIΔα protein expressed in CHO cells (Figure S1).

### 3.2 | TFPIα-deficient mice lack platelet TFPI activity and have normal plasma TFPI and TAT levels

TFPI activity in platelets was assessed using assays measuring activation of FX by TF-FVIIa.[28] Platelet lysates prepared from *Tfpi*$^{+/+}$ mice had 16.4 ± 5.0 fmoles TFPIα/mg protein while platelet lysates prepared from *Tfpi*$^{\Delta\alpha/\Delta\alpha}$ mice had 1.1 ± 0.5 fmoles TFPIα/mg protein (Figure 2A). Adding a TFPI antibody to platelet lysates from *Tfpi*$^{+/+}$ mice resulted in the expected decrease in TFPI activity, reducing it to the same level as in *Tfpi*$^{\Delta\alpha/\Delta\alpha}$ platelet lysates. Adding the same antibody to lysates prepared from *Tfpi*$^{\Delta\alpha/\Delta\alpha}$ platelets had no effect indicating that the TFPI activity detected was background for the assay. These results (1) confirm that normally there is active TFPI in platelets and (2) show that it is absent in the *Tfpi*$^{\Delta\alpha/\Delta\alpha}$ mice.

Figure 2B and C compare TFPI activity and antigen in plasma obtained from *Tfpi*$^{+/+}$ and *Tfpi*$^{\Delta\alpha/\Delta\alpha}$ mice. No significant differences were observed between the two genotypes, consistent with previous observations that little or no TFPIα is normally present in mouse plasma.

Finally, plasma TAT complex levels were measured to determine whether lack of TFPIα tilts the global hemostatic balance toward greater thrombin production. Again, no differences were observed between *Tfpi*$^{+/+}$ and *Tfpi*$^{\Delta\alpha/\Delta\alpha}$ mice (Figure 3). Taken together, the results in Figures 2 and 3 confirm that TFPIα is the predominant TFPI isoform in platelets and that suppressing TFPIα expression has no effect on circulating TFPI or TAT levels.

### 3.3 | TFPIα and the hemostatic response *in vivo*

Two previously characterized models were used to measure the contribution of TFPIα during the hemostatic response to injury. In the first model, the jugular vein in *Tfpi*$^{+/+}$ and *Tfpi*$^{\Delta\alpha/\Delta\alpha}$ mice was surgically exposed and punctured with a 30-gauge needle (300 μm diameter).[44] The time until bleeding cessation was noted and the vein segment containing the injury was excised and opened, allowing the hemostatic plug that had formed to be examined from the intraluminal and extraluminal perspectives using confocal and two-photon fluorescence imaging followed by scanning electron microscopy.

Intraluminal views of the injury 5 min after penetration showed large aggregates of minimally activated platelets with little if any fibrin visible (Figure 4A–C). The extraluminal

views of the same injury sites showed highly activated platelets expressing surface P-selectin and an abundant amount of fibrin (Figure 4D–F). These hemostatic plugs were similar to those we have reported previously.[44] Platelet deposition, platelet activation and fibrin accumulation were quantified by measuring CD41 (platelet-associated) fluorescence, P-selectin mean fluorescence intensity within the CD41 volume, and fibrin sum fluorescence intensity (Figure 5A–C). P-selectin expression was used as a marker for α-granule secretion. Fibrin accumulation was used a surrogate for thrombin activity. There were no discernible differences in platelet accumulation, activation, or fibrin formation between the $Tfpi^{+/+}$ and $Tfpi^{\Delta\alpha/\Delta\alpha}$ mice. Notably, however, the $Tfpi^{\Delta\alpha/\Delta\alpha}$ mice had a slightly shortened jugular vein bleeding time compared with $Tfpi^{+/+}$ mice (mean and standard deviation: 108 ± 14 s vs. 71 ± 7 s; $p = .0273$; Figure 5D).

In the second injury model, the hemostatic response was observed in real-time using confocal fluorescence microscopy following a penetrating laser injury in cremaster muscle arterioles.[43,51] Platelet accumulation (CD41), P-selectin surface expression, and fibrin deposition were examined. The results obtained in the $Tfpi^{+/+}$ mice were consistent with those that we and others have reported previously. There was a rapid accumulation of platelets that peaked after approximately 90 s and a more gradual accumulation of fibrin. P-selectin appearance on the surface of the platelets increased more slowly, reaching about one-half of the platelet area by the end of the period of observation (Figure 6). Removing TFPIα had no apparent effect: platelet accumulation, P-selection expression, and fibrin formation were the same in $Tfpi^{+/+}$ and $Tfpi^{\Delta\alpha/\Delta\alpha}$ mice (Figure 6B).

## 4 | DISCUSSION

TFPI is the major anticoagulant protein regulating TF-initiated thrombin generation during the hemostatic response to vascular damage. Full-length TFPIα is a more effective anticoagulant than its C-terminally truncated forms when soluble protein is added to plasma coagulation assays.[20] It is also the only isoform that contains 3 Kunitz-type domains, all of which along with the C-terminus enable optimal inhibition of TF-FVIIa, FXa, and early prothrombinase activity.[4,19,20] Even though platelets contain only 5% to 10% of circulating TFPI, the platelet pool consists exclusively of full-length TFPIα[28] and therefore contributes to TFPI anticoagulant activity in human blood.[27]

Although there are species differences in the TFPI concentration in plasma, the TFPIα isoform is evolutionarily conserved. In both humans and mice, TFPIα is the only isoform present in platelets and megakaryocytes.[27,28] The observation that TFPIα is present in platelets and megakaryocytes, but TFPIβ is not, suggests that platelet-borne TFPI is synthesized by megakaryocytes and possibly by platelets, but is not taken up from plasma.[28] The location of TFPIα within platelets has been the subject of investigation, as has its release during platelet activation. Platelet TFPIα does not colocalize with platelet α-granule or lysosome markers, suggesting that it is contained in neither structure. Stimulation of platelets with thrombin and other agonists causes TFPIα release.[27,28,52] In addition, at least some TFPIα can be detected moving to the platelet surface or into the 200 000*g* supernatant when platelets are strongly stimulated by a combinations of thrombin and convulxin or thrombin and a $Ca^{++}$ ionophore.[28]

Given that there is already ample TFPI in plasma and on endothelial cells, what role is played by TFPIα in general and platelet TFPIα in particular? Our hypothesis was that TFPIα released by platelets directly at a site of injury would have an outsized role in limiting thrombin production. Here, we tested this hypothesis by studying the hemostatic response to injury in mice with a selective deficiency in TFPIα. Mice that are TFPI null die with evidence of a consumptive coagulopathy[1] and defects in cerebrovascular development.[53] In contrast, we found that *Tfpi*$^{\Delta\alpha/\Delta\alpha}$ mice are viable, fertile, and born in the expected numbers from heterozygous *Tfpi*$^{+/\Delta\alpha}$ crosses. Although they lack platelet TFPI, they have normal plasma TFPI levels. This finding is consistent with mice expressing transgenic TFPIα under control of the GP1bα promoter, which have a four- to fivefold increase in platelet TFPIα, but normal plasma TFPI levels.[54] Notably, the *Tfpi*$^{\Delta\alpha/\Delta\alpha}$ mice did not have increased plasma TAT complex levels indicating that the absence of TFPIα did not produce a systemic increase in inappropriate thrombin production.

To further assess the impact of removing TFPIα, we studied the hemostatic response *in vivo* in detail. Platelet and fibrin accumulation at a site of vascular injury does more than simply seal a breach in a damaged vessel wall. It also produces a modified local environment in which the movement of plasma-borne molecules is greatly restricted.[55–57] This allows proteins secreted by platelets to accumulate at higher concentrations than they would otherwise, and allows thrombin generated at the site of injury or on the surface of platelets to reach higher local concentrations.[58] Our hypothesis was that platelet-derived TFPIα would become available locally to limit thrombin production and that removing it would permit greater local thrombin production. This in turn could lead to greater platelet and fibrin accumulation, without necessarily producing a systemic increase in TAT levels. Because conditions vary considerably in different parts of the vasculature, we examined the hemostatic response in both the macrovasculature (the jugular vein) and the microvasculature (arterioles in the cremaster muscle circulation) using models that have been presented previously.[43,44]

The results show that platelet accumulation, platelet activation, and fibrin accumulation occur to the same extent in the presence and absence of TFPIα. In the microcirculation, where we were able to observe the hemostatic response in real-time, we found no differences in the kinetics or extent of the response. Of note, a previous study by Crawley et al. found that infusing a TFPI antibody that is not isoform selective into Bambi$^{-/-}$ mice, which have a defect in fibrin accumulation after injury, restores both fibrin accumulation and thrombus stability in an injury model similar to the one that we used.[59] Combined with our results in which only TFPIα is missing, this suggests that plasma TFPIγ and endothelial cell TFPIβ, or a combination of TFPIα, TFPIβ, and TFPIγ, are the relevant isoforms in this setting.

The results we obtained in the jugular vein were somewhat different. Direct observation of the exposed jugular vein allows the time to bleeding cessation to be measured in the same vessel in which we were then able to observe the hemostatic structure that resulted from the injury. Here, we found that bleeding ceased faster in the mice missing TFPIα. However, although statistically significant, this difference was small and we did not observe differences in the structure of hemostatic thrombi 5 min after injury. There was also no evidence of a prothrombotic state in the mice missing TFPIα compared with wild-type,

which was measured as no difference in TAT levels. Thus, despite the significant shortening of the bleeding time, we conclude that in both the micro- and the macrocirculation the contribution of TFPIα to a normal hemostatic response in mice is minimal.

How do these results fit with those reported previously? As noted in the Introduction, Maroney et al. examined the impact of removing TFPI from hematopoietic cells by transplanting *Tfpi*$^{-/-}$ fetal liver cells into irradiated heterozygous *Tfpi*$^{+/-}$ recipient mice.[41] Loss of hematopoietic TFPI led to an increase in platelet accumulation after an electrolytic injury in the femoral vein and carotid artery. It also caused a reduction in the tail bleeding time and an increase in fibrin accumulation after electrolytic injury in mice that lacked both FVIII and hematopoietic TFPI.[42] However, *Tfpi*$^{+/-}$ mice have one-half the normal amount of plasma TFPI.[41,42] This difference from the mice studied here, along with irradiation and the use of hemostatic injuries rather than prothrombotic injuries, may account for the differences that we observed compared with those earlier studies.

In conclusion, the present studies show that TFPIα, which is mostly in platelets, is not uniquely essential for normal murine hemostasis when plasma TFPI concentrations are otherwise normal. The absence of TFPIα shortened the bleeding time following puncture of the jugular vein suggesting that release of TFPIα from platelets at the site of vascular injury has some impact on the hemostatic response, but the effect was small. In addition to TFPIα, platelets contain two other anticoagulant proteins, Protein S (PS) and Protease Nexin-1 (PN-1),[60] which may partially compensate for TFPIα anticoagulant activity in the hemostasis assays performed here. PS and PN-1 are also released at the site of vascular injury and their absence decreases blood loss in various bleeding models.[61–63] Because TFPIα, PS, and PN-1 act at different points in the coagulation cascade, they likely work in concert following release from activated platelets to dampen localized thrombin generation and prevent intravascular thrombotic events.

## Supplementary Material

Refer to Web version on PubMed Central for supplementary material.

## ACKNOWLEDGMENTS

We thank Andrea Stout and the Cell and Developmental Biology Microscopy Core at the University of Pennsylvania for assistance with two-photon and scanning electron microscopy imaging. The authors gratefully acknowledge research funding from the National Institutes of Health (P01 HL146373, P01 HL040387, P01 HL139420) and an Early Career Investigator Award from the Bayer Hemophilia Awards Program (to M.T.). This work was supported by the National Institutes of Health (HL068835 [A.E.M.]). A.E.S. was supported by training grant HL007209.

### Funding information

Foundation for the National Institutes of Health, Grant/Award Number: HL007209, HL068835, P01 HL040387, P01 HL139420 and P01 HL146373; Bayer, Grant/Award Number: Bayer Hemophilia Awards Program (to M.T.)

### CONFLICT OF INTEREST

Dr. Mast receives research funding from Novo Nordisk and has received honoraria for serving on Novo Nordisk Advisory Boards. The other authors have declared that no conflict of interest exists.

## REFERENCES


1. Huang ZF, Higuchi D, Lasky N, et al. Tissue factor pathway inhibitor gene disruption produces intrauterine lethality in mice. Blood. 1997;90(3):944–951. [PubMed: 9242522]
2. Baugh RJ, Broze GJ Jr, Krishnaswamy S. Regulation of extrinsic pathway factor Xa formation by tissue factor pathway inhibitor. J Biol Chem. 1998;273(8):4378–4386. [PubMed: 9468488]
3. Wood JP, Ellery PER, Maroney SA, Mast AE. Biology of tissue factor pathway inhibitor. Blood. 2014;123(19):2934–2943. [PubMed: 24620349]
4. Wood JP, Bunce MW, Maroney SA, Tracy PB, Camire RM, Mast AE. Tissue factor pathway inhibitor-alpha inhibits prothrombinase during the initiation of blood coagulation. Proc Natl Acad Sci U S A. 2013;110(44):17838–17843. [PubMed: 24127605]
5. Monkovic DD, Tracy PB. Activation of human factor V by factor Xa and thrombin. Biochemistry. 1990;29(5):1118–1128. [PubMed: 2322551]
6. Monković DD, Tracy PB. Functional characterization of human platelet-released factor V and its activation by factor Xa and thrombin. J Biol Chem. 1990;265(28):17132–17140. [PubMed: 2211616]
7. Broze GJ Jr, Girard TJ. Factor V, tissue factor pathway inhibitor, and east Texas bleeding disorder. J Clin Invest. 2013;123(9):3710–3712. [PubMed: 23979154]
8. Vincent LM, Tran S, Livaja R, Bensend TA, Milewicz DM, Dahlbäck B. Coagulation factor V(A2440G) causes east Texas bleeding disorder via TFPIα. J Clin Invest. 2013;123(9):3777–3787. 10.1172/JCI69091. [PubMed: 23979162]
9. Ndonwi M, Girard TJ, Broze GJ Jr. The C-terminus of tissue factor pathway inhibitor α is required for its interaction with factors V and Va. J Thromb Haemost. 2012;10(9):1944–1946. [PubMed: 22738072]
10. Cunha ML, Bakhtiari K, Peter J, Marquart JA, Meijers JCM, Middeldorp S. A novel mutation in the F5 gene (factor V Amsterdam) associated with bleeding independent of factor V procoagulant function. Blood. 2015;125(11):1822–1825. [PubMed: 25634741]
11. Maroney SA, Ferrel JP, Collins ML, Mast AE. Tissue factor pathway inhibitor-gamma is an active alternatively spliced form of tissue factor pathway inhibitor present in mice but not in humans. J Thromb Haemost. 2008;6(8):1344–1351. [PubMed: 18503630]
12. Chang JY, Monroe DM, Oliver JA, Roberts HR. TFPIbeta, a second product from the mouse tissue factor pathway inhibitor (TFPI) gene. Thromb Haemost. 1999;81(1):45–49. [PubMed: 9974373]
13. Zhang J, Piro O, Lu L, Broze GJ. Glycosyl phosphatidylinositol anchorage of tissue factor pathway inhibitor. Circulation. 2003;108(5):623–627. [PubMed: 12835228]
14. Chang JY, Monroe D, Oliver J, Liles D, Roberts H. Cloning, expression, and characterization of mouse tissue factor pathway inhibitor (TFPI). Thromb Haemost. 1998;79(2):306–309. [PubMed: 9493581]
15. Wun TC, Kretzmer KK, Girard TJ, Miletich JP, Broze GJ. Cloning and characterization of a cDNA coding for the lipoprotein-associated coagulation inhibitor shows that it consists of three tandem Kunitz-type inhibitory domains. J Biol Chem. 1988;263(13):6001–6004. [PubMed: 2452157]
16. Maroney SA, Ellery PE, Wood JP, Ferrel JP, Martinez ND, Mast AE. Comparison of the inhibitory activities of human tissue factor pathway inhibitor (TFPI)α and TFPIβ. J Thromb Haemost. 2013;11(5):911–918. 10.1111/jth.12188. [PubMed: 23480518]
17. Ndonwi M, Tuley EA, Broze GJ Jr. The Kunitz-3 domain of TFPI-alpha is required for protein S-dependent enhancement of factor Xa inhibition. Blood. 2010;116(8):1344–1351. [PubMed: 20479289]
18. Hackeng TM, Sere KM, Tans G, Rosing J. Protein S stimulates inhibition of the tissue factor pathway by tissue factor pathway inhibitor. Proc Natl Acad Sci U S A. 2006;103(9):3106–3111. [PubMed: 16488980]
19. Peraramelli S, Suylen DPL, Rosing J, Hackeng TM. The Kunitz 1 and Kunitz 3 domains of tissue factor pathway inhibitor are required for efficient inhibition of factor Xa. Thromb Haemost. 2012;108(2):266–276. [PubMed: 22627666]

20. Wesselschmidt R, Likert K, Girard T, Wun TC, Broze GJ Jr. Tissue factor pathway inhibitor: the carboxy-terminus is required for optimal inhibition of factor Xa. Blood. 1992;79(8):2004–2010. [PubMed: 1562726]
21. Girard TJ, Tuley E, Broze GJ Jr. TFPIβ is the GPI-anchored TFPI isoform on human endothelial cells and placental microsomes. Blood. 2012;119(5):1256–1262. [PubMed: 22144186]
22. Broze GJ Jr, Girard TJ. Tissue factor pathway inhibitor: structure-function. Front Biosci (Landmark Ed). 2012;17:262–280. [PubMed: 22201743]
23. Maroney SA, Ferrel JP, Pan S, White TA, Simari RDd, Mcvey JH, Mast AE. Temporal expression of alternatively spliced forms of tissue factor pathway inhibitor in mice. J Thromb Haemost. 2009;7(7):1106–1113. [PubMed: 19422457]
24. Bajaj MS, Kuppuswamy MN, Manepalli AN, Bajaj SP. Transcriptional expression of tissue factor pathway inhibitor, thrombomodulin and von Willebrand factor in normal human tissues. Thromb Haemost. 1999;82(3):1047–1052. [PubMed: 10494762]
25. Bajaj MS, Kuppuswamy MN, Saito H, Spitzer SG, Bajaj SP. Cultured normal human hepatocytes do not synthesize lipoprotein-associated coagulation inhibitor: evidence that endothelium is the principal site of its synthesis. Proc Natl Acad Sci U S A. 1990;87(22):8869–8873. [PubMed: 2247459]
26. Werling RW, Zacharski LR, Kisiel W, Bajaj SP, Memoli VA, Rousseau SM. Distribution of tissue factor pathway inhibitor in normal and malignant human tissues. Thromb Haemost. 1993;69(4):366–369. [PubMed: 8497849]
27. Novotny WF, Girard TJ, Miletich JP, Broze GJ Jr. Platelets secrete a coagulation inhibitor functionally and antigenically similar to the lipoprotein associated coagulation inhibitor. Blood. 1988;72(6):2020–2025. [PubMed: 3143429]
28. Maroney SA, Haberichter SL, Friese P, et al. Active tissue factor pathway inhibitor is expressed on the surface of coated platelets. Blood. 2007;109(5):1931–1937. [PubMed: 17082321]
29. Novotny WF, Girard TJ, Miletich JP, Broze GJ. Purification and characterization of the lipoprotein-associated coagulation inhibitor from human plasma. J Biol Chem. 1989;264(31):18832–18837. [PubMed: 2553722]
30. Broze GJ Jr, Girard TJ, Novotny WF. Regulation of coagulation by a multivalent Kunitz-type inhibitor. Biochemistry. 1990;29(33):7539–7546. [PubMed: 2271516]
31. van der Logt CP, Dirven RJ, Reitsma PH, Bertina RM. Expression of tissue factor and tissue factor pathway inhibitor in monocytes in response to bacterial lipopolysaccharide and phorbolester. Blood Coagul Fibrinolysis. 1994;5(2):211–220. [PubMed: 8054453]
32. Caplice NM, Mueske CS, Kleppe LS, Peterson TE, Broze GJ, Simari RD. Expression of tissue factor pathway inhibitor in vascular smooth muscle cells and its regulation by growth factors. Circ Res. 1998;83(12):1264–1270. [PubMed: 9851943]
33. Novotny WF, Palmier M, Wun TC, Broze GJ Jr, Miletich JP. Purification and properties of heparin-releasable lipoprotein-associated coagulation inhibitor. Blood. 1991;78(2):394–400. [PubMed: 2070077]
34. Girard TJ, Grunz K, Lasky NM, Malone JP, Broze GJ. Re-evaluation of mouse tissue factor pathway inhibitor and comparison of mouse and human tissue factor pathway inhibitor physiology. J Thromb Haemost. 2018;16(11):2246–2257. [PubMed: 30194803]
35. Sandset PM, Abildgaard U, Larsen ML. Heparin induces release of extrinsic coagulation pathway inhibitor (EPI). Thromb Res. 1988;50(6):803–813. [PubMed: 3413731]
36. Novotny WF, Brown SG, Miletich JP, Rader DJ, Broze GJ Jr. Plasma antigen levels of the lipoprotein-associated coagulation inhibitor in patient samples. Blood. 1991;78(2):387–393. [PubMed: 2070076]
37. Dahm A, van Hylckama Vlieg A, Bendz B, Rosendaal F, Bertina RM, Sandset PM. Low levels of tissue factor pathway inhibitor (TFPI) increase the risk of venous thrombosis. Blood. 2003;101(11):4387–4392. [PubMed: 12560220]
38. Kaiser B, Glusa E, Hoppensteadt DA, Breddin HK, Amiral J, Fareed J. A supersulfated low-molecular-weight heparin (IK-SSH) increases plasma levels of free and total tissue factor pathway inhibitor after intravenous and subcutaneous administration in humans. Blood Coagul Fibrinolysis. 1998;9(6):517–523. [PubMed: 9819002]

39. White TA, Witt TA, Pan S, et al. Tissue factor pathway inhibitor overexpression inhibits hypoxia-induced pulmonary hypertension. Am J Respir Cell Mol Biol. 2010;43(1):35–45. [PubMed: 19648471]
40. Wood JP, Petersen HH, Yu B, Wu X, Hilden I, Mast AE. TFPIα interacts with FVa and FXa to inhibit prothrombinase during the initiation of coagulation. Blood Adv. 2017;1(27):2692–2702. [PubMed: 29291252]
41. Maroney SA, Cooley BC, Ferrel JP, Bonesho CE, Mast AE. Murine hematopoietic cell tissue factor pathway inhibitor limits thrombus growth. Arterioscler Thromb Vasc Biol. 2011;31(4):821–826. [PubMed: 21233452]
42. Maroney SA, Cooley BC, Ferrel JP, et al. Absence of hematopoietic tissue factor pathway inhibitor mitigates bleeding in mice with hemophilia. Proc Natl Acad Sci U S A. 2012;109(10):3927–3931. [PubMed: 22355108]
43. Stalker TJ, Traxler EA, Wu J, et al. Hierarchical organization in the hemostatic response and its relationship to the platelet-signaling network. Blood. 2013;121(10):1875–1885. [PubMed: 23303817]
44. Tomaiuolo M, Matzko CN, Poventud-Fuentes I, Weisel JW, Brass LF, Stalker TJ. Interrelationships between structure and function during the hemostatic response to injury. Proc Natl Acad Sci U S A. 2019;116(6):2243–2252. [PubMed: 30674670]
45. Dawlaty MM, van Deursen JM. Gene targeting methods for studying nuclear transport factors in mice. Methods. 2006;39(4):370–378. [PubMed: 16887365]
46. White TA, Johnson T, Zarzhevsky N, et al. Endothelial-derived tissue factor pathway inhibitor regulates arterial thrombosis but is not required for development or hemostasis. Blood. 2010;116(10):1787–1794. [PubMed: 20516367]
47. Pan S, White TA, Witt TA, Chiriac A, Mueske CS, Simari RD. Vascular-directed tissue factor pathway inhibitor overexpression regulates plasma cholesterol and reduces atherosclerotic plaque development. Circ Res. 2009;105(7):713–720. [PubMed: 19713537]
48. White TA, Pan S, Witt TA, Simari RD. Murine strain differences in hemostasis and thrombosis and tissue factor pathway inhibitor. Thromb Res. 2010;125(1):84–89. [PubMed: 19398123]
49. Ellery PE, Maroney SA, Cooley BC, et al. A balance between TFPI and thrombin-mediated platelet activation is required for murine embryonic development. Blood. 2015;125(26):4078–4084. 10.1182/blood-2015-03-633958. [PubMed: 25954015]
50. Maroney SA, Cunningham AC, Ferrel J, et al. A GPI-anchored co-receptor for tissue factor pathway inhibitor controls its intracellular trafficking and cell surface expression. J Thromb Haemost. 2006;4(5):1114–1124. [PubMed: 16689766]
51. Falati S, Gross P, Merrill-Skoloff G, Furie BC, Furie B. Real-time in vivo imaging of platelets, tissue factor and fibrin during arterial thrombus formation in the mouse. Nat Med. 2002;8(10):1175–1181. [PubMed: 12244306]
52. Winckers K, Thomassen S, Cate HT, Hackeng TM. Platelet full length TFPI-alpha in healthy volunteers is not affected by sex or hormonal use. PLoS One. 2017;12(2):e0168273. [PubMed: 28158181]
53. Maroney SA, Westrick RJ, Cleuren AC, et al. Tissue factor pathway inhibitor is required for cerebrovascular development in mice. Blood. 2021;137:258–268. [PubMed: 32735640]
54. Siebert AE, Maroney SA, Martinez ND, Mast AE. Intrauterine lethality in Tfpi gene disrupted mice is differentially suppressed during mid- and late-gestation by platelet TFPIα overexpression. J Thromb Haemost. 2021;19:1483–1492. [PubMed: 33728763]
55. Welsh JD, Stalker TJ, Voronov R, et al. A systems approach to hemostasis: 1. The interdependence of thrombus architecture and agonist movements in the gaps between platelets. Blood. 2014;124(11):1808–1815. [PubMed: 24951424]
56. Tomaiuolo M, Stalker TJ, Welsh JD, Diamond SL, Sinno T, Brass LF. A systems approach to hemostasis: 2. Computational analysis of molecular transport in the thrombus microenvironment. Blood. 2014;124(11):1816–1823. [PubMed: 24951425]
57. Stalker TJ, Welsh JD, Tomaiuolo M, et al. A systems approach to hemostasis: 3. Thrombus consolidation regulates intrathrombus solute transport and local thrombin activity. Blood. 2014;124(11):1824–1831. [PubMed: 24951426]

58. Welsh JD, Colace TV, Muthard RW, Stalker TJ, Brass LF, Diamond Sl. Platelet-targeting sensor reveals thrombin gradients within blood clots forming in microfluidic assays and in mouse. J Thromb Haemost. 2012;10(11):2344–2353. [PubMed: 22978514]

59. Crawley JTB, Zalli A, Monkman JH, et al. Defective fibrin deposition and thrombus stability in Bambi(−/−) mice are mediated by elevated anticoagulant function. J Thromb Haemost. 2019;17(11):1935–1949. [PubMed: 31351019]

60. Siebert AE, Mast AE. Platelet anticoagulant proteins: Modulators of thrombosis propensity within a procoagulant cell. J Thromb Haemost. 2020;18:2083–2086. [PubMed: 32729671]

61. Boulaftali Y, Adam F, Venisse L, et al. Anticoagulant and antithrombotic properties of platelet protease nexin-1. Blood. 2010;115(1):97–106. [PubMed: 19855083]

62. Aymonnier K, Kawecki C, Venisse L, et al. Targeting protease nexin-1, a natural anticoagulant serpin, to control bleeding and improve hemostasis in hemophilia. Blood. 2019;134(19):1632–1644. [PubMed: 31383642]

63. Calzavarini S, Prince-Eladnani R, Saller F, et al. Platelet protein S limits venous but not arterial thrombosis propensity by controlling coagulation in the thrombus. Blood. 2020;135(22):1969–1982. [PubMed: 32276277]

## Essentials

- Tissue factor pathway inhibitor alpha (TFPIα) is the isoform in platelets and its role in hemostasis is unknown.
- Transgenic mice with a defect in TFPIα expression were generated and characterized.
- Hemostatic plugs formed in the micro- or macrovasculature showed no changes in platelet or fibrin accumulation.
- The vascular injury models studied indicate TFPIα is not essential for normal hemostatic response in mice.

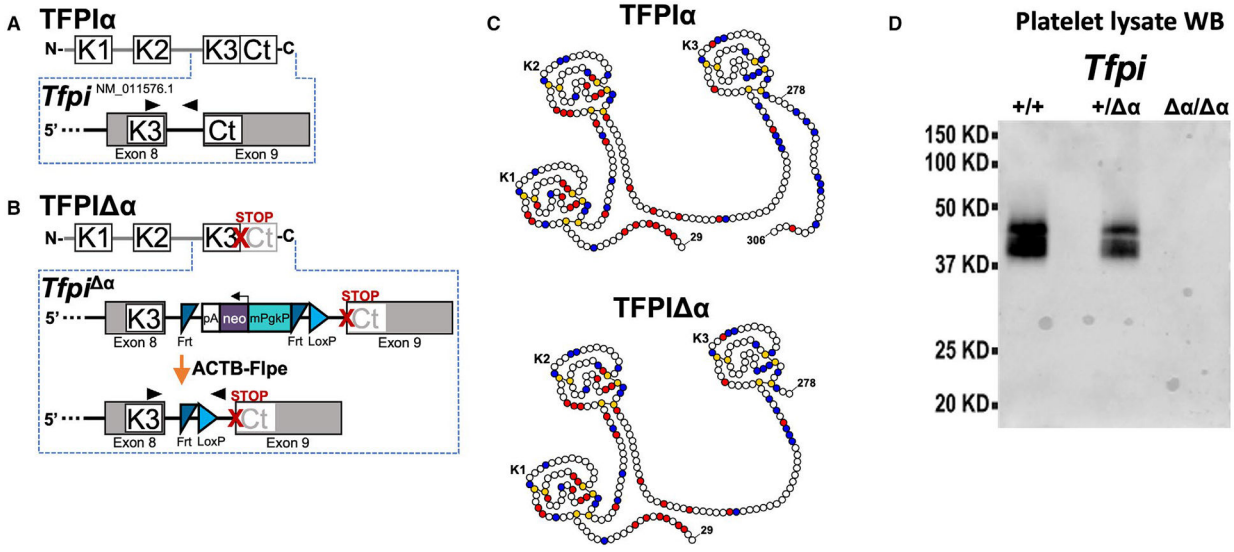


**FIGURE 1.**

Schematic representation of TFPI gene disruption in mice. (A) Schematic of wild-type TFPIα depicting the three tandem Kunitz-type inhibitor domains (K1, K2, and K3), adjacent linker regions (gray line), and the basic C-terminus (Ct). Lower inset is a schematic of the corresponding genomic region and exonic (gray boxes) and intronic (black line) regions of the *Tfpi* transcript variant (NCBI RefSeq accession: NM_011576.1) encoding K3 and the C-terminal tail of TFPIα. (B) Predicted schematic of the truncated TFPIΔα protein product (upper) and the corresponding targeted mutation within the *Tfpi* genomic locus (lower). Insertion of the targeting construct into the mouse *Tfpi* gene incorporated an in-frame premature stop codon (red X) by replacing nucleotides 835 through 837 within the *Tfpi*α coding sequence at the 5′-end of the terminal exon (c.835–837delins*, exon 9 of NM_011576.1) that encodes the C-terminal tail of TFPIα. Mice harboring this construct were crossed to ACTB-Flpe mice to remove the neo-cassette. Arrowheads in (A and B) depict the position of genotyping primers. (C) Diagrams of the protein structures of TFPIα and C-terminal deleted TFPIα (TFPIΔα) showing the Kunitz domains (K1-K3) and the highly basic C-terminus. Red, blue, and yellow circles indicate acidic residues, basic residues, and cysteine residues. (D) Western blot analysis of TFPI from platelet lysate under nonreducing conditions. This experiment was performed twice with identical results indicating no TFPIα in platelet lysates from $Tfpi^{\Delta\alpha/\Delta\alpha}$ mice. The presence of a doublet band may reflect differential glycosylation of platelet TFPIα or nonspecific proteolysis during platelet lysis and sample processing, even though a protease inhibitor cocktail was used during platelet lysis.[23] C, carboxyl group; N, amine group; TFPI, tissue factor pathway inhibitor

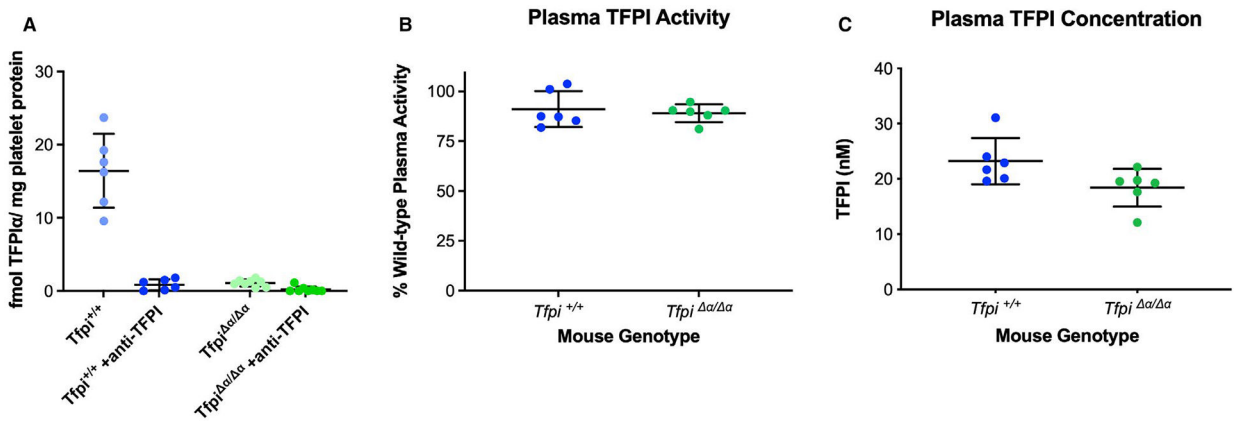


**FIGURE 2.**

TFPIα-deficient mice lack platelet TFPI activity with no effect on plasma TFPI. (A) TFPI activity in platelet lysates prepared from *Tfpi*$^{+/+}$ and *Tfpi*$^{\Delta\alpha/\Delta\alpha}$ mice was measured by its ability to inhibit FXa generation by TF-FVIIa. Where indicated, 100 μg/ml of polyclonal anti-mouse TFPI antibody was added to the assay mix to inhibit TFPI. Lysates from *Tfpi*$^{+/+}$ platelets, but not *Tfpi*$^{\Delta\alpha/\Delta\alpha}$ platelets or *Tfpi*$^{+/+}$ platelets spiked with anti-TFPI, had TFPI activity and inhibited FXa generation. When analyzed by ANOVA followed by Tukey's multiple comparison test, the TFPI activity was significantly higher in the *Tfpi*$^{+/+}$ platelet lysate ($p < .0001$) with no differences between the other three groups. (B) Plasma TFPI activity in samples obtained from *Tfpi*$^{+/+}$ and *Tfpi*$^{\Delta\alpha/\Delta\alpha}$ mice detected by its ability to inhibit TF-FVIIa initiated FXa generation. The groups were not different when analyzed by two-tailed *t*-test. (C) Plasma TFPI antigen concentration in samples obtained from *Tfpi*$^{+/+}$ and *Tfpi*$^{\Delta\alpha/\Delta\alpha}$ mice. The groups were not different when analyzed by two-tailed *t*-test. Data are presented as a mean ± SD. Each point represents the average of 4 technical replicates of a platelet lysate sample that was pooled from two mice of the same genotype. F, factor; TFPI, tissue factor pathway inhibitor

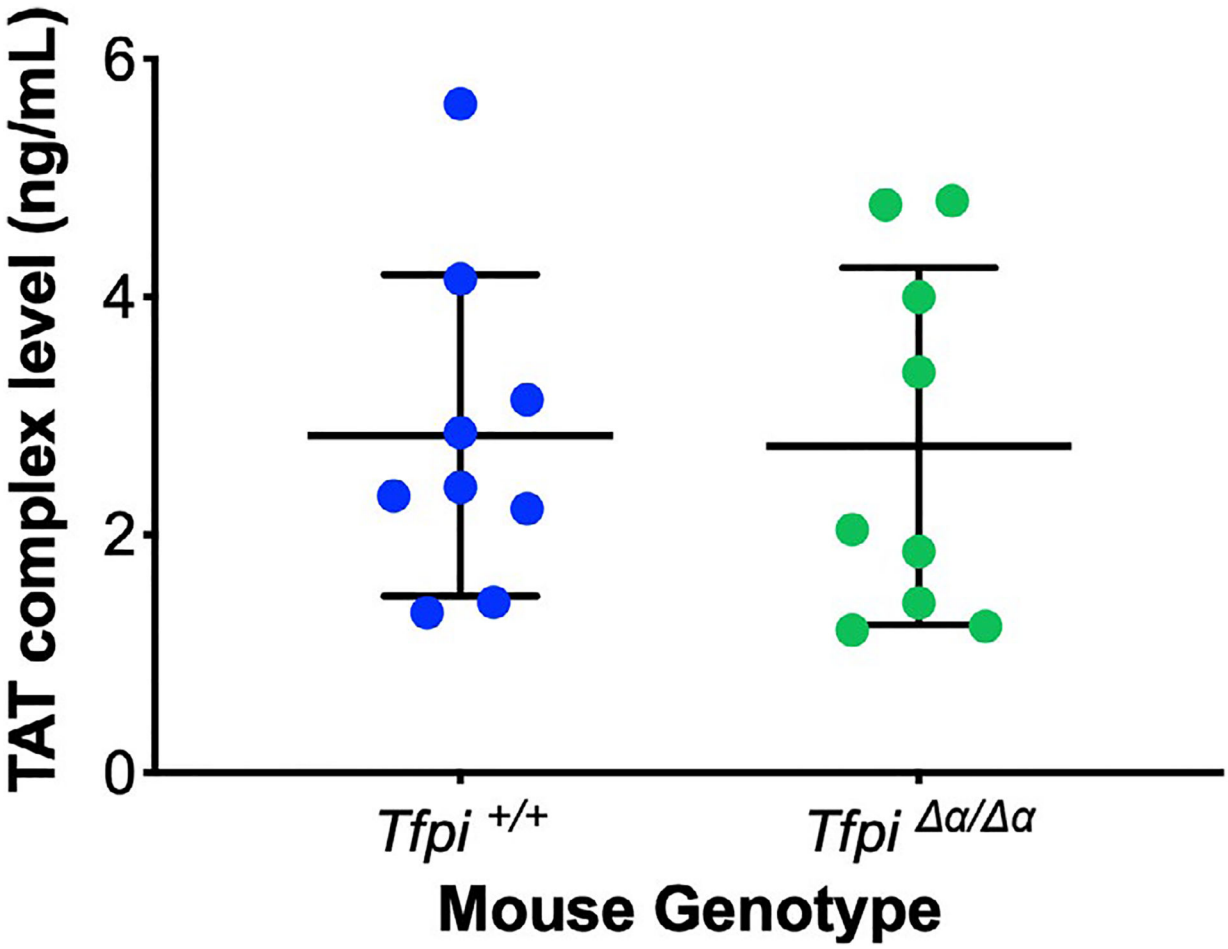


**FIGURE 3.**

Plasma thrombin-antithrombin complex levels. Plasma thrombin-antithrombin (TAT) complex levels were measured by ELISA in plasma obtained from *Tfpi*$^{+/+}$ and *Tfpi*$^{\Delta\alpha/\Delta\alpha}$ mice. The groups were not different when analyzed by two-tailed *t*-test. Data are presented as mean ± SD

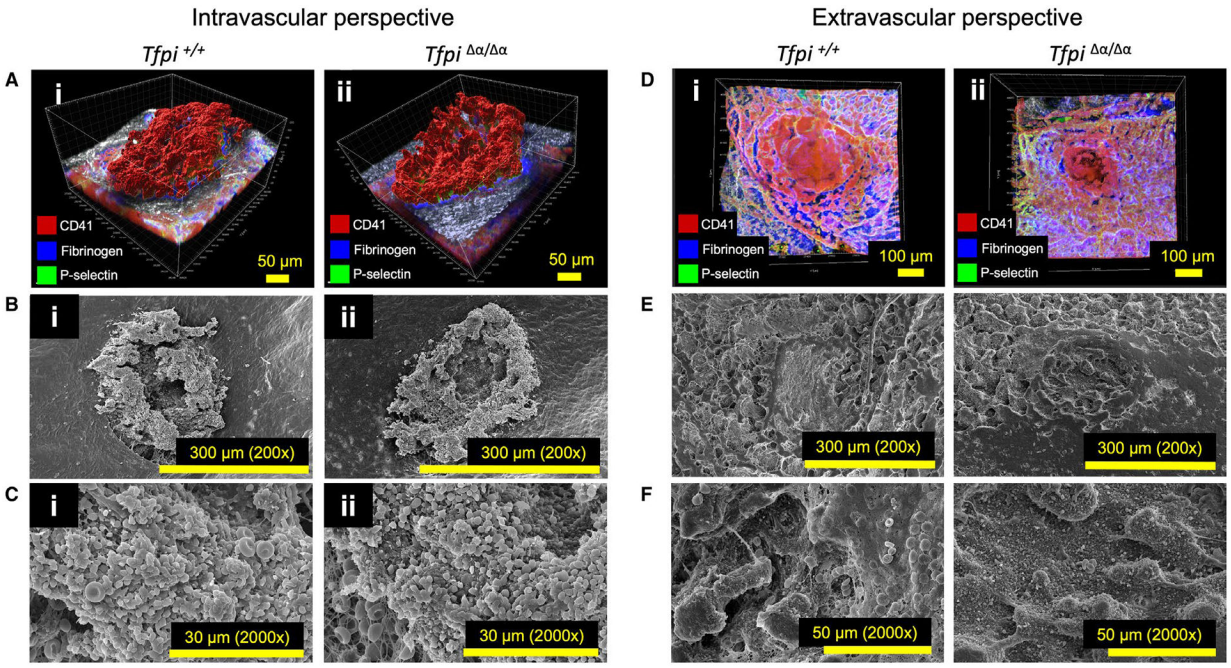


**FIGURE 4.**

Hemostatic response in the jugular vein. (A) Representative 3-dimensional reconstructions of fluorescence images of the side view of the intravascular side of a hemostatic plug 5 min following a puncture injury in an exposed jugular using a 300-μm-diameter needle. (representative of 14–17 hemostatic plugs imaged from the intravascular side). (i) *Tfpi*$^{+/+}$ and (ii) *Tfpi*$^{\Delta\alpha/\Delta\alpha}$ mice with platelets (CD41), P-selectin, and fibrin shown in the colors indicated. (B and C) Scanning electron images of the hemostatic plugs in A (B = 200×, C = 2000×) show that the intravascular surface of the hemostatic plugs is mainly composed of platelets that are minimally activated in appearance. There are no striking differences between the *Tfpi*$^{+/+}$ and (ii) *Tfpi*$^{\Delta\alpha/\Delta\alpha}$ mice. (D) Representative 3-dimensional reconstructions of fluorescence images from the top view of the extravascular side of jugular vein hemostatic plugs from (i) *Tfpi*$^{+/+}$ and (ii) *Tfpi*$^{\Delta\alpha/\Delta\alpha}$ mice (representative of 10–16 hemostatic plugs imaged from the extravascular side). (E and F) Scanning electron images of the hemostatic plugs in D (E = 200×, F = 2000×) show that the external surface of the hemostatic plugs is composed of activated platelets and abundant fibrin deposition with no evident differences between the *Tfpi*$^{+/+}$ and (ii) *Tfpi*$^{\Delta\alpha/\Delta\alpha}$ mice

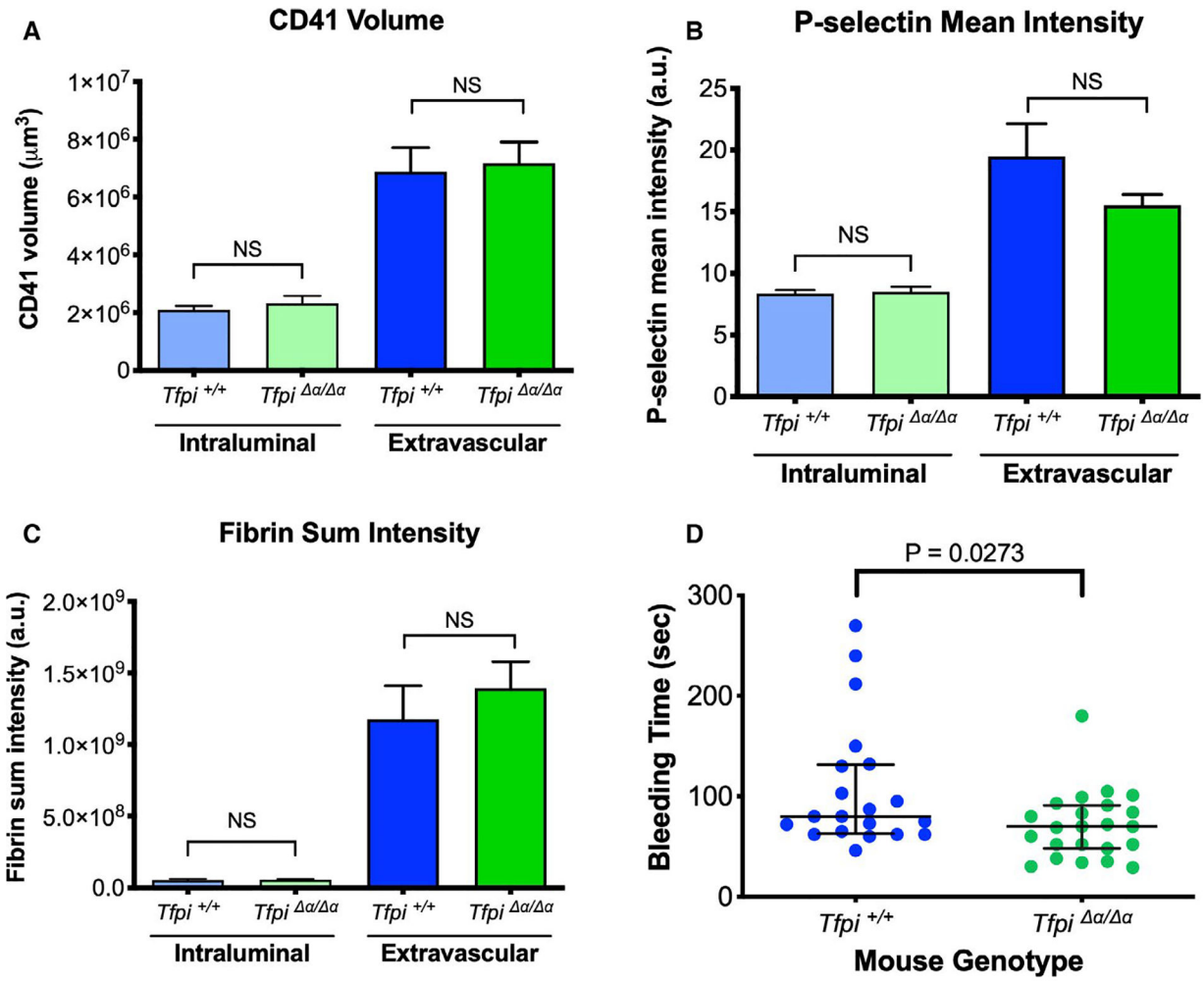


**FIGURE 5.**

Quantification of hemostatic response following jugular vein puncture injury. The fluorescence of hemostatic plugs, such as those shown in Figure 4, were quantified from the intraluminal and extravascular sides. The total volume of platelet accumulation (A), P-selectin mean fluorescence intensity within the CD41 volume (B) and fibrin sum fluorescence intensity (C) was determined in $Tfpi^{+/+}$ ($n$ = 10–14) and $Tfpi^{\Delta\alpha/\Delta\alpha}$ ($n$ = 16–17) mice. The graphs show mean ± standard error of the mean (SEM). Statistical analysis used Welch's test using $p \leq .05$ for significance. (D) The bleeding time from a jugular puncture injury in $Tfpi^{+/+}$ ($n$ = 20) and $Tfpi^{\Delta\alpha/\Delta\alpha}$ ($n$ = 23) mice was determined as 108 ± 14 s and 71 ± 7 s, respectively. The graphs indicate median and interquartile range

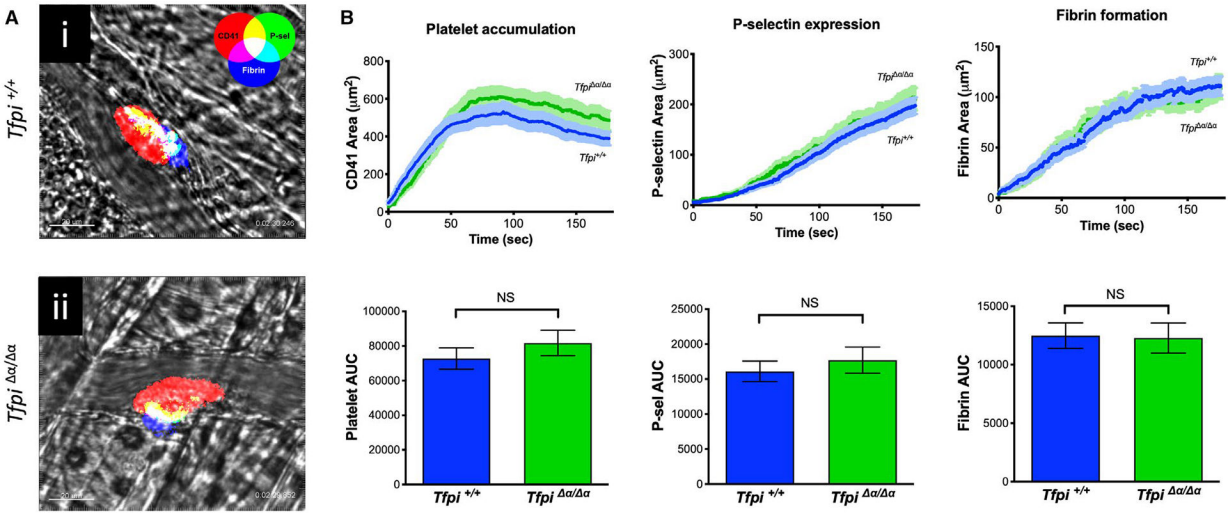


**FIGURE 6.**

Hemostatic response in the microcirculation. (A) Representative images of hemostatic plug formation 3 min after laser injury in *Tfpi*$^{+/+}$ and *Tfpi*$^{\Delta\alpha/\Delta\alpha}$ mouse cremaster muscle arterioles. Platelet accumulation (CD41) is shown in red, P-selectin exposure is in green, and fibrin formation is in blue. (B) Time course of platelet accumulation, P-selectin exposure, and fibrin deposition in *Tfpi*$^{+/+}$ (blue) and *Tfpi*$^{\Delta\alpha/\Delta\alpha}$ (green) mice. Data are expressed as mean area ± SEM; *Tfpi*$^{+/+}$ mice, $n = 72$ laser injuries in 5 mice; *Tfpi*$^{\Delta\alpha/\Delta\alpha}$ mice, $n = 63$ laser injuries in 6 mice. Statistics were calculated based on the area under each curve. Analysis used the Mann-Whitney test with $p < .05$ deemed significant

## TABLE 1

TFPI genotype of weanlings from *Tfpi*$^{+/\Delta\alpha}$ × *Tfpi*$^{+/\Delta\alpha}$ mating[a]

| TFPI genotype | Number (*n* = 426) | Observed (%) | Expected (%) |
|---|---|---|---|
| *Tfpi* $^{+/+}$ | 110 | 25.8 | 25 |
| *Tfpi* $^{+/\Delta\alpha}$ | 224 | 52.6 | 50 |
| *Tfpi* $^{\Delta\alpha/\Delta\alpha}$ | 92 | 21.6 | 25 |

TFPI, tissue factor pathway inhibitor.

[a]Statistical analysis was performed using the $\chi^2$ test and $p \leq .05$ as significant. By this criterion, none of the differences between genotypes reached significance.

## TABLE 2

Hematological parameters[a]

| Features | *Tfpi* $^{+/+}$ | *Tfpi* $^{\Delta\alpha/\Delta\alpha}$ |
|---|---|---|
| Red blood cells (M/(μl) | 9.25 ± 0.45 | 9.67 ± 0.58 |
| Hemoglobin (g/dl) | 14.2 ± 0.7 | 14.6 ± 0.4 |
| Hematocrit (%) | 43.1 ± 2.4 | 45.1 ± 1.6 |
| Platelets (K/μl) | 877 ± 142 | 881 ± 264 |
| Mean platelet volume (fl) | 5.9 ± 0.1 | 5.9 ± 0.2 |
| White blood cells (K/μl) | 14.1 ± 3.7 | 14.3 ± 3.2 |
| Neutrophils (%) | 37.5 ± 20.2 | 45.5 ± 19.0 |
| Lymphocytes (%) | 58.9 ± 19.9 | 50.5 ± 19.0 |
| Monocytes (%) | 0.5 ± 0.4 | 0.3 ± 0.2 |
| Eosinophils (%) | 3.0 ± 0.4 | 3.6 ± 0.5 |
| Basophils (%) | 0.0 ± 0.1 | 0.1 ± 0.0 |

[a]Data shown are the mean ± SD for blood obtained from 8- to 12-week-old *Tfpi*$^{+/+}$ ($n = 7$) and *Tfpi*$^{\Delta\alpha/\Delta\alpha}$ ($n = 6$) mice. Statistical analysis was performed by Mann-Whitney test and $p \leq .05$ as significant. By this criterion, none of the differences between genotypes reached significance.